ELSEVIER

Surface Science 406 (1998) 103–116

surface science

Silicide formation at palladium surfaces. Part I: Crystalline and amorphous silicide growth at the Pd(110) surface

Elisabeth Kampshoff, Nicolas Wälchli, Klaus Kern *

Institut de Physique Expérimentale, EPFL, CH-1015 Lausanne, Switzerland

Received 2 June 1997; accepted for publication 14 January 1998

Abstract

Si adsorption and silicide formation at the Pd(110) surface is studied by scanning tunneling microscopy and vibrational spectroscopy of adsorbed CO. The CO stretch vibration is shown to be sensitive to the local bonding arrangement on the heterogeneous Si/Pd(110) surface. Silicide growth shows a rich temperature-dependent behavior determined by the competition between interdiffusion and chemical reaction. At low temperatures ($T<140$ K), amorphous Si is grown on the surface. Above this temperature, silicide formation is observed. Initially amorphous silicide clusters and above 320 K well-shaped crystalline silicide islands are formed. The growth mode of the silicide is of the Stranski–Krastanov type at $T\geq 500$ K. The crystalline silicide is found to be a metastable phase of Pd_2Si. The grown silicide is unstable at elevated temperatures and decays with lifetimes varying from several minutes to hours. A structural model for the crystalline silicide is presented. © 1998 Elsevier Science B.V. All rights reserved.

Keywords: Growth; Infrared absorption spectroscopy; Metal–semiconductor interfaces; Palladium; Scanning tunneling microscopy; Silicon

1. Introduction

Silicon–metal interfaces attract particular interest due to their critical importance in semiconductor device technology. A microscopic understanding of the contact reaction between Si and the metal to form silicide is of pratical and fundamental interest, and numerous studies have been reported in the last 30 years [1,2]. These studies have in common that they focus on the adsorption of metal atoms on Si substrates. Only little is known about the counterpart, i.e. the chemisorption and reaction of Si on metal surfaces [3–9]. In the few studies reported so far, it has been observed that the deposition of silicon on metals usually leads to the formation of poorly ordered alloys. Crystalline silicide phases are the exception, and have only been found on Cu surfaces [7,8]. In addition, for some systems strong asymmetries in the interfacial intermixing between the metal and silicon and between silicon and the metal have been observed [9]. To understand the initial stages of Schottky barrier formation, it is important to establish whether the poor ordering and the asymmetry in the interface morphology and chemistry is a general feature or whether it is material-specific. This requires more systematic studies of the morphology and chemistry of well-defined silicon–metal systems. We have thus begun a series of experimental studies exploring the very early stages of interface formation in silicon deposition on single-crystal surfaces of palladium.

* Corresponding author. Fax: (+41) 21 6933604

0039-6028/98/$19.00 © 1998 Elsevier Science B.V. All rights reserved.
PII: S0039-6028(98)00104-6

In the present paper, we report our results for the Pd(110) surface.

The Si/Pd system has been chosen because its counterpart, the Pd/Si system, is one of the most thoroughly studied systems. The adsorption of Pd at Si substrates has been studied with particular emphasis on silicide formation. From an experimental point of view the system is attractive, since in general only one single reaction product, Pd_2Si, is formed at Si substrates below $T=1000$ K [1,10]. Under some extreme growth conditions, such as fast heat treatment by a high-energy electron beam or laser pulses, different palladium silicide compounds can also be created [11]. Soft post-annealing of the grown silicide films confirms that Pd_2Si is the only stable phase. The epitaxial condition between the basal plane of the Pd_2Si and the Si(111) surface (lattice misfit of less than 2%) allows the growth of crystalline silicide films on Si(111) at annealing temperatures above $T \geq 600$ K [10,12,13].

The silicide formation enthalpy of $H \approx 1.3$ eV involves energy contributions of the interfacial reaction step in addition to mass transport [14–17]. The growth process of thick palladium silicide films follows a parabolic law, indicating that the rate-limiting step is interdiffusion through the silicide layer rather than interfacial reaction. In contrast to the very slow process of film growth, the initial step of silicide formation proceeds considerably more quickly [12,18–22]. Spontaneous Pd_2Si formation within 3–25 Å of the initial interface is already observed at room temperature. It is assumed that the heat of adsorption of Pd on Si provides sufficient energy to spontaneously promote the initial step of silicide formation also at very low deposition temperatures ($T \geq 180$ K) [20].

The purpose of the present work is to give a detailed description of the surface morphology and reactivity of Si deposited on Pd(110) as a function of the deposition temperature ($100\ \text{K} \leq T \leq 600\ \text{K}$) and as a function of the Si dosage. We are basically interested in the contact reaction as the initial step of silicide formation, and restrict ourselves to Si coverages $\theta_{Si} \leq 4$ ML. We will demonstrate that silicide formation in both systems, i.e. Pd deposited on Si and Si deposited on Pd, is similar. The systems are extremely reactive. Silicide reaction on the Pd(110) surface already occurs at a deposition temperature of 140 K, with the formation of amorphous Pd_2Si clusters. Whereas on Si substrates only amorphous Pd_2Si is observed upon Pd deposition below ≈ 600 K, we will show that at temperatures slightly above room temperature the Pd(110) substrate promotes the growth of a metastable crystalline silicide phase.

Si/Pd(110) surface characterisation is performed by an in-situ combination of scanning tunneling microscopy (STM) and reflection absorption infrared spectroscopy (RAIRS) of adsorbed CO. We profit from the possibility of correlating surface chemical analysis with atomic-level surface structure investigation. As a chemical sensor we use the CO molecule which is adsorbed at the heterogeneous surfaces. The internal stretch vibration, which is easily accessible with RAIRS, reacts quite sensitively to the chemical nature of its surrounding, and is thus a valuable probe of the local surface chemical composition.

2. Experimental

The experiments were performed in an ultrahigh vacuum chamber combining in-situ reflection absorption infrared spectroscopy (RAIRS) and scanning tunnelling microscopy (STM) with standard facilities for surface preparation and surface quality control. The apparatus is described in detail in Ref. [23]. It is divided into two main chambers, a preparation chamber and an analysis chamber. The Pd(110) surface was prepared by several cycles of Ar^+ sputtering at 700 K, annealing in an oxygen atmosphere of 1×10^{-6} mbar at 600 K and flash annealing to 900 K. Si evaporation on the well-prepared surfaces was performed by electron-bombardment heating of a Si rod in a commercial evaporator. The deposition rate was $R_{Si} \approx 6 \times 10^{-4}$ ML s^{-1}. Calibration of the deposition rate was performed by means of STM and RAIR spectroscopy of adsorbed CO at $T=100$ K. At low coverages, the Si growth is found to be two-dimensional, and the IR signal of Si bound CO is used as a direct measure of the Si dosage, assuming a sticking coefficient of 1. The Si/Pd(110) surfaces were transferred from the preparation

chamber to the STM position as well as to the RAIRS position in the analysis chamber by a long-travel manipulator without breaking the ultrahigh vacuum. The surface morphology was imaged with a home-built Besocke-type STM operating in the temperature range $100\,K \leq T \leq 600\,K$. All STM measurements were performed in the constant-current mode at a positive or negative tip bias of 0.2–1.0 V and tunnelling currents below 2.0 nA. The infrared measurements were performed with a commercial Fourier-transform spectrometer (FTIR, Mattson 6020). For metal substrates, a reflection geometry with an angle of incidence of 80° is chosen. CO was adsorbed on the Si/Pd(110) surface at 100 K, and a monolayer coverage of CO was achieved after a dosage of ~20 Langmuirs. The infrared spectra were recorded at a resolution of 8 cm^{-1}.

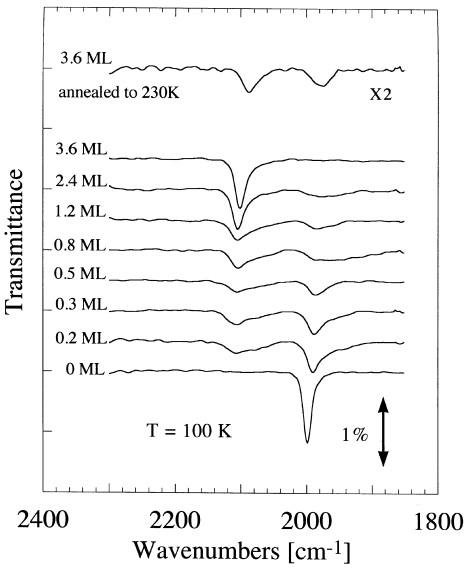

Fig. 1. Infrared spectra of a monolayer of CO adsorbed on Si/Pd(110) after Si deposition at 100 K. The Si dosage is indicated in the figure. The topmost spectrum shows the infrared spectrum of the remaining CO after annealing the surface covered with 3.6 ML Si at 230 K.

3. Results

3.1. From amorphous Si to amorphous silicide ($100\,K \leq T \leq 300\,K$)

Si deposition at 100 K is non-reactive, and small Si clusters are formed at the Pd(110) surface. Fig. 1 shows a series of infrared spectra of CO adsorbed on the Si/Pd(110) surface as a function of the Si dosage. At the bottom, a reference spectrum of a monolayer of CO adsorbed on pure Pd(110) is presented. The single absorption band at 2000 cm^{-1} is due to the infrared absorption of CO molecules adsorbed in short bridge positions over adjacent Pd substrate atoms [24–27]. At full CO coverage, a p2mg overlayer is revealed: the CO molecules are ordered in zig-zag chains running along the $[\bar{1}10]$ direction of the substrate. Upon Si deposition, a second absorption band appears around 2104 cm^{-1}. With increasing Si dosage this band gains in intensity, whereas the intensity of the original band at 2000 cm^{-1} decreases. A considerable line-broadening as well as a small red-shift of the low-frequency band is clearly observed, indicating that the patches of the remaining Pd substrate become smaller and are randomly distributed. At a Si dosage of 3.6 ML, the infrared signal of CO/Pd(110) vanishes completely, leaving a single adsorption at 2104 cm^{-1} with a line width of 16 cm^{-1}. Since there are no hints of Pd atoms mixed in with the topmost layer, we conclude that the surface is completely terminated with Si which did not react with the Pd substrate. Thus the band at 2104 cm^{-1} must be assigned to CO adsorbed on amorphous Si (a-Si). In addition, no frequency shift is observed in the studied Si coverage range, indicating that Si adsorption at a deposition temperature of $T=$ 100 K is also non-reactive at low Si coverages. The peak maximum is close to the frequency observed for CO adsorbed on Si(100)-(2×1) (2081 cm^{-1}) [28]. It is reasonable to assume a similar adsorption geometry, i.e. an upright bridge position on top of adjacent Si atoms.

Silicide formation becomes evident in the infrared spectra on annealing the CO/Si/Pd(110) sample. The topmost spectrum in Fig. 1 was measured after annealing a monlayer of CO adsorbed on 3.6 ML Si to 230 K. The spectrum has to be compared to the spectrum just below it. The total infrared intensity is reduced by a factor of 2, indicating that approximately 50% of the CO

molecules have already desorbed at $T \leq 230$ K. This result is not surprising, since the desorption temperature for CO from Si(100)-(2×1) is known to be 220 K [28]. The high-frequency mode is shifted to 2090 cm^{-1}. A second band appears at 1990 cm^{-1}, indicating the presence of Pd atoms mixed with Si atoms in the topmost layer. In agreement with the results of Ref. [20], we conclude that the initial step in silicide formation, the contact reaction, is already activated below 230 K at the Si/Pd(110) interface. Detailed AES analysis confirms this result. Above 140 K a multiple peak shape has already developed around 92 eV which is characteristic of palladium silicide formation [10].

At temperatures between 140 and 320 K, the silicide formed at the Pd(110) surface is amorphous. On the right-hand side of Fig. 2 we show two STM images representing the surface morphology after Si deposition at room temperature. In the low coverage range, small silicide clusters are formed at the surface. They have an average size of 10–40 Å and are randomly distributed at the surface. These clusters are quite similar to the amorphous structures observed at the Pd/Si(111) surface after submonolayer Pd deposition at room temperature [18]. With increasing Si deposition, the clusters grow in size and the surface becomes more rough. The diffuse LEED image indicates a non-crystalline surface structure.

On the left-hand side of Fig. 2 the corresponding series of CO absorption spectra are shown as a function of Si dosage. The bottom spectrum again reveals the single absorption band at 2000 cm^{-1} of a monlayer of CO adsorbed on pure Pd(110). Si deposition at 300 K first becomes obvious in the appearance of a very broad high-frequency mode at 2090 cm^{-1}. Note that the same frequency has been observed as a consequence of silicide formation upon annealing a Si/Pd(110) surface prepared at 100 K, as shown in the topmost spectrum of Fig. 1. The band must be attributed to CO adsorbed on amorphous silicide. The relatively broad line reflects the inhomogenity of the grown film. With increasing Si dosage the intensity of this band increases over the original band at

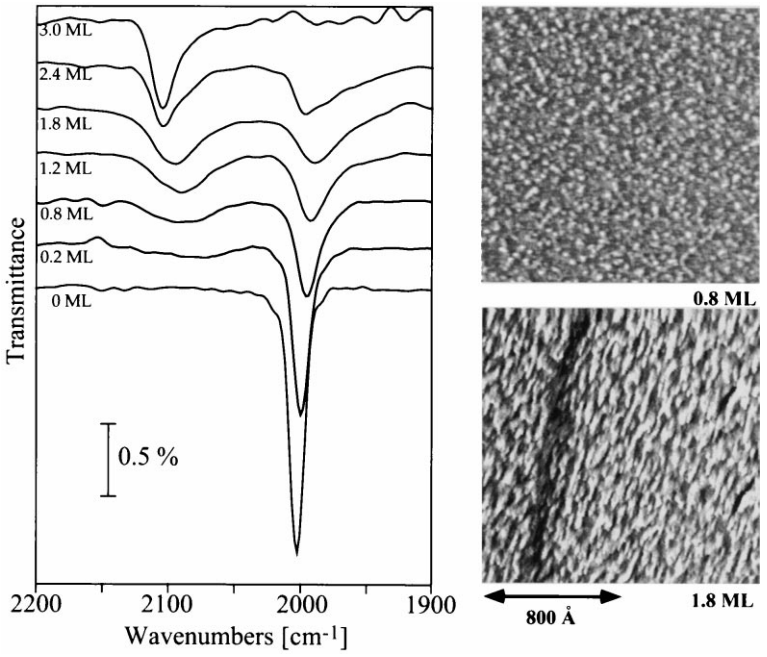

Fig. 2. Left: infrared absorption spectra of a monolayer of CO adsorbed on Si/Pd(110) after Si deposition at 300 K as a function of the Si dosage. 40 L CO was dosed to the surface at 100 K. Right: STM images showing the surface morphology of Si/Pd(110) after Si deposition at 300 K. Si dosage: 0.8 ML (top), 1.8 ML (bottom).

2000 cm^{-1}. Attention must be drawn to the intensity maximum of the 2090 cm^{-1} mode at a Si dosage of $\sim\theta=1.8$ ML. With further increasing coverage, an important upward shift to 2104 cm^{-1} is observed. This frequency characterises the absorption of CO on a-Si, therefore indicating the presence of unreacted Si in the topmost surface layer. The amount of unreacted Si increases with Si dosage, and at $\theta=3$ ML the surface is completely Si-terminated. At room temperature, only a very few layers of palladium silicide are obviously sufficient to block the diffusion of Si and Pd completely, and silicide formation is stopped. This phenomenon is known from Pd deposition on Si substrates in connection with "under-reaction" conditions, where Pd enrichment is observed in the topmost layer [12,20].

Fig. 3 shows the relative infrared intensities of the absorption band at 2000 cm^{-1} of CO adsorbed at Pd sites of the heterogeneous Si/Pd(110) surface as a function of the Si dosage. The experimental data for Si deposition at 1000, 300 and 550 K all decrease with increasing Si dosage, indicating a change in adsorption site of adsorbed CO due to the coadsorption of Si at the surface. A fit to the data for $T=100$ K in the low-coverage regime ($\theta<0.5$ ML) is also presented (dashed line). The essentially linear behavior indicates that initially, Si growth upon deposition at 100 K is two-dimensional. A significant change in the slope of the curve ($T=100$ K) is observed at higher Si dosages ($\theta\geq0.5$ ML), indicating the onset of three-dimensional growth.

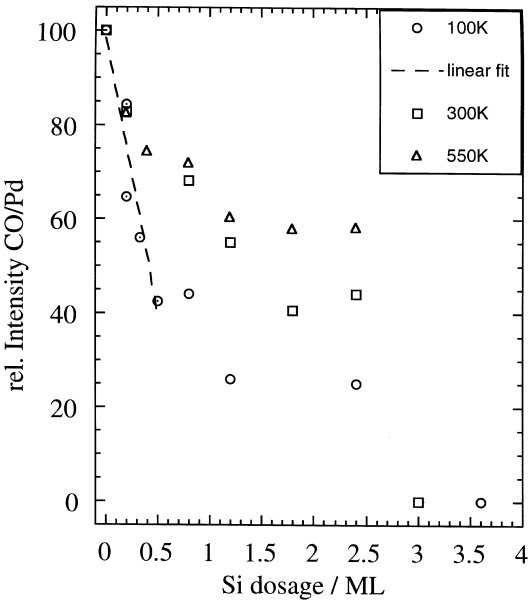

Fig. 3. Relative infrared intensities of the absorption band of CO adsorbed on Pd in the bridge position as a function of the Si dosage at three Si deposition temperatures: ○ $T=100$ K, □ $T=300$ K, △ $T=550$ K.

The data characterising Si deposition at $T=100$ K show a monotonous decrease. In contrast, the data representing epitaxially grown silicide upon Si depositon at $T=550$ K show a pronounced intensity plateau above a Si dosage of $\theta\approx1.2$ ML. A constant Pd concentration in the topmost layer is inferred, which is characteristic of a completely mixed monolayer. The saturation intensity is $\sim60\%$, indicating that about 40% of adsorbed CO has changed its adsorption site due to silicide formation in the topmost layer. We conclude that on the Pd(110) surface, a Pd_2Si-like compound is formed. Although silicide formation is observed upon Si deposition at $T=300$ K, the corresponding data in Fig. 3 do not show a pronounced saturation behaviour. This is consistent with the Si enrichment of the topmost layer at a Si dosage exceeding $\theta\geq1.8$ ML, as already observed in Fig. 2. Due to the "under-reaction" conditions revealed at room temperature, the amount of unreacted Si in the topmost layer increases with the Si dosage, ending up with a completely Si-terminated surface above $\theta=3$ ML.

3.2. Crystalline silicide ($T\geq320$ K)

At temperatures above $T=320$ K, the reaction scenario is quite different. As an example we show in Fig. 4 two STM images characterising silicide formation at 350 K after deposition of 0.1 ML and silicide formation at 400 K after deposition of 0.6 ML. In Fig. 5 a series of six STM images is presented showing silicide formation at 550 K as a function of Si deposition. The silicide islands formed in the temperature range between 350 and 600 K all have the same crystalline structure. They grow epitaxially on the Pd(110) substrate, as

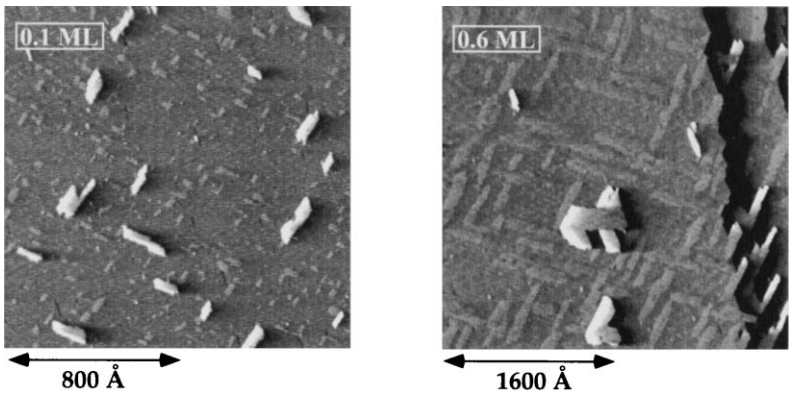

Fig. 4. STM images showing the surface morphology of Si/Pd(110) after Si deposition at 350 K (left, Si dosage 0.1 ML) and 400 K (right, Si dosage 0.6 ML).

indicated by a sharp $\begin{pmatrix} 1 & 1 \\ 4 & 0 \end{pmatrix}$ LEED superstructure with two domains (see Fig. 6).

As is clearly visible in Fig. 4, two kinds of well-shaped silicide islands are formed upon Si deposition at 350 and 400 K, one embedded in the first Pd layer and the other on the Pd(110) surface, one step height above. Both island types have a rhomboidal shape. There are two domains visible which are oriented along the diagonal $[\bar{1}12]$ and $[\bar{1}1\bar{2}]$ directions of the Pd(110) surface unit cell. The adislands and the embedded islands show the same distinct orientation. From the STM measurements, a silicide island height of 1.7 Å is inferred.

The embedded silicide islands are formed by the direct reaction of Pd in the surface layer with impinging Si atoms, whereas the adislands are formed through the reaction of ejected Pd adatoms with impinging Si adatoms. The source of ejected Pd adatoms is most probably an exchange process between the Si atoms with the Pd atoms of the substrate layer [29]. This kind of exchange process plays an important role in binary surface alloy formation since it creates the possibility for foreign atoms to penetrate the substrate and create a mixed surface atom composition [30]. The density of the embedded silicide islands is much higher than that of the adislands. This can be understood easily, because the flux of Si atoms arriving at the Pd surface is larger than the "effective flux" of Pd adatoms ejected onto the surface. The nucleation probability of the embedded silicide islands is thus higher than the probability that Si and Pd adatoms meet and nucleate an adisland.

With increasing temperature, migration becomes increasingly faster with respect to depositon, i.e. the nucleation density decreases and only few very large embedded silicide islands grow (Fig. 5). The migration length exceeds the average terrace length, and silicide formation starts at step edges. Each single terrace is interspersed with elongated islands growing from the upper step edge into the terrace (Fig. 5a). Note that each terrace is exclusively covered with one single type of silicide domain, indicating that the direction of the step edge is decisive in domain nucleation (Fig. 5a–d). Only for thicker silicide films does this influence become less important, and both domains are equally distributed on a single terrace (Fig. 5d).

The STM images in Fig. 5 reveal a Stranski–Krastanov growth mode for silicide formation on the Pd(110) surface. The silicide monolayer is complete ($\theta \leq 1.2$ ML, Fig. 5a) before three-dimensional growth sets in. The silicide islands in the second layer grow in the form of adislands starting from the step edges and growing on top of the terrace (Fig. 5c1). Except for a small number of silicide islands nucleating on top of the first and second layers, the step flow mode is still dominant at $\theta = 1.8$ ML. The effect of three-dimensional growth is most pronounced in the STM image of Fig. 5d, where islands in the second (grey patches) and third layers (white patches) are clearly

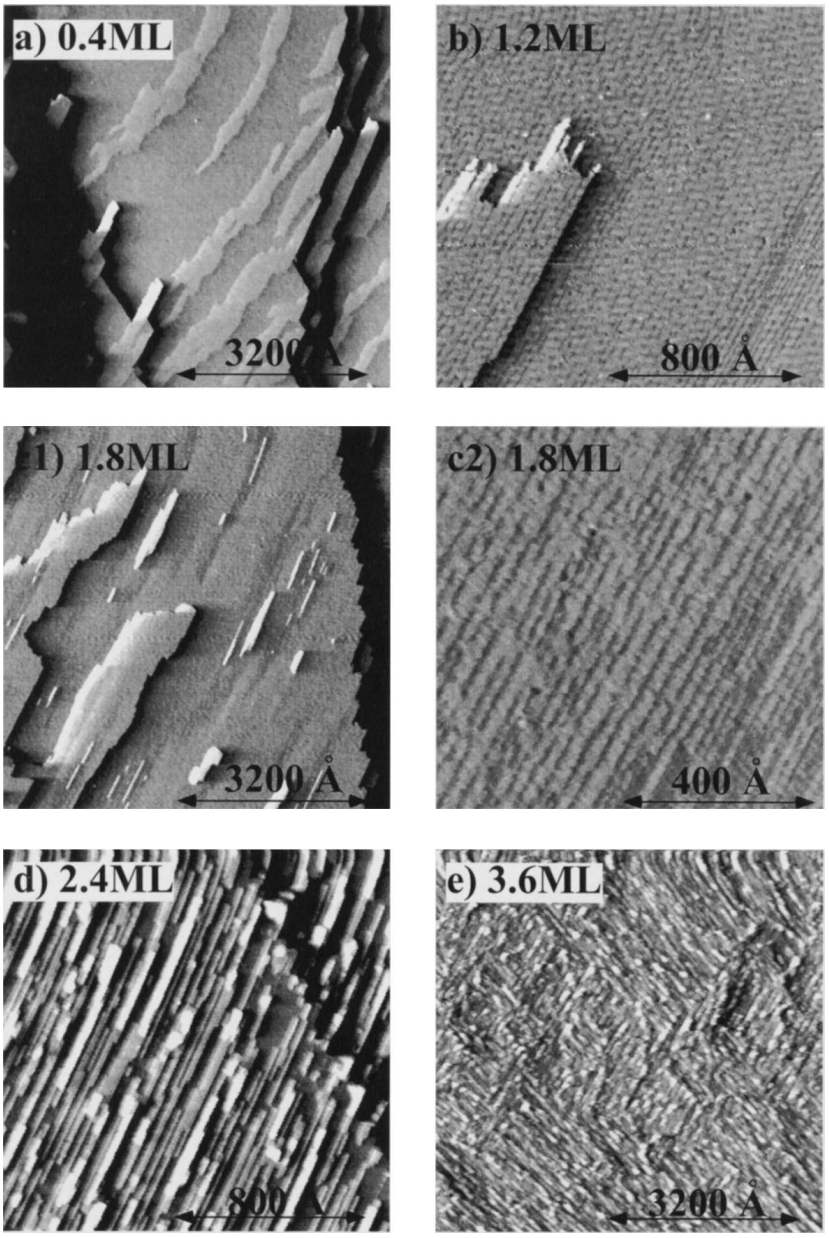

Fig. 5. STM images showing the surface morphology of Si/Pd(110) after Si deposition at 550 K at the indicated Si dosage. (c2) is an enlargement of (c1), clearly indicating the pattern of dark stripes which are interpreted as misfit dislocations.

visible as well as small patches of the first silicide layer.

A pattern of parallel dark stripes visible on the silicide islands grown at 550 K attracts particular attention (Fig. 5b and c2). The depression stripes running along the [$\bar{1}$12] direction are $\sim$9 Å in width and have an average separation of $\sim$45 Å. We identify these stripes as misfit dislocations partially relieving the strain. The silicide must thus be under substantial compressive strain, and

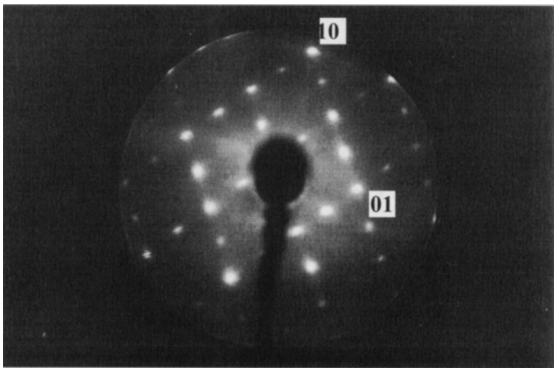

Fig. 6. LEED pattern of crystalline silicide grown upon deposition of 0.6 ML Si at $T=400$ K on Pd(110). The sample was cooled to 100 K for the LEED measurement (electron energy 55 eV).

islands can only grow coherently up to a critical size. Larger islands have to relieve their strain by the introduction of misfit dislocations. The LEED measurements reveal the same $\begin{pmatrix}1 & 1\\ 4 & 0\end{pmatrix}$ pattern with additional spot splittings along the diagonals, indicating that the silicide between the misfit dislocations has the same crystalline structure as the coherent islands grown at 350 and 400 K.

The infrared spectra of CO adsorbed on the crystalline silicide are shown in Fig. 7. The morphology of the corresponding heterogeneous Si/Pd(110) surfaces was shown in Fig. 5. The bottom spectrum, characterising a deposit of 0.2 ML at 550 K, is dominated by an absorption band around 2000 cm^{-1} due to CO adsorbed on the Pd atoms in the bridge position. A second broad absorption around 2074 cm^{-1} indicates the presence of Si in the surface. With increasing Si deposition, the high-frequency band sharpens considerably and gains in intensity over the band at 2000 cm^{-1}. Saturation is obvious at a Si dosage of $\theta \approx 1.2$ ML, corresponding to the completion of the first silicide monolayer. The dominant adsorption species on the crystalline silicide monolayer is CO, which is bound to two adjacent Pd atoms (see Fig. 2). Its absorption frequency does not change with respect to the clean Pd(110) substrate, consistent with the negligible charge transfer observed in silicide formation [31]. Crystalline silicide formation is evident by comparing the spectra with the analogous spectrum of amorphous Si on

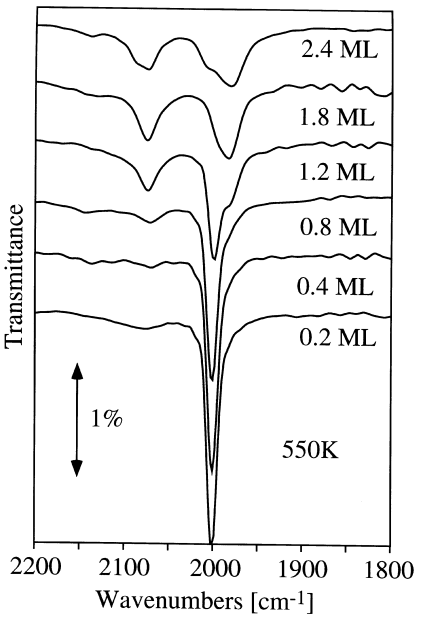

Fig. 7. Infared absorption spectra of a monolayer of CO adsorbed on Si/Pd(110) after Si deposition at 550 K as a function of the Si dosage. The Si dosage is indicated in the figure. A monolayer was achieved with a dosage of 40 L CO.

Pd(110) in Fig. 1 and amorphous silicide on Pd(110) in Fig. 2. The peak maximum of the high-frequency mode at 2074 cm^{-1} is shifted by 30 cm^{-1} with respect to unreactive Si deposition at 100 K, and by 14 cm^{-1} with respect to amorphous silicide formation at room temperature. At $\theta=1.2$ ML a small shoulder is visible at 2080 cm^{-1}, indicating the onset of silicide growth in the second layer. With increasing Si deposition this band dominates the original absorption at 2000 cm^{-1}. This frequency indicates a Pd bridge configuration. In the Byholder model of CO bonding at metal surfaces [32], the chemical red-shift of 20 cm^{-1} indicates an increased charge density at the Pd atoms in the second silicide layer. At $\theta=2.4$ ML a small shoulder at 2104 cm^{-1} appears, indicating the unreactive growth of Si in the topmost layer.

A valuable complement to the site assignment is CO adsorption spectroscopy. The bottom spectrum of Fig. 8 was taken after CO adsorption at 150 K on a Si/Pd(110) surface prepared at 400 K with $\theta=2.4$ ML. It is quite similar to the

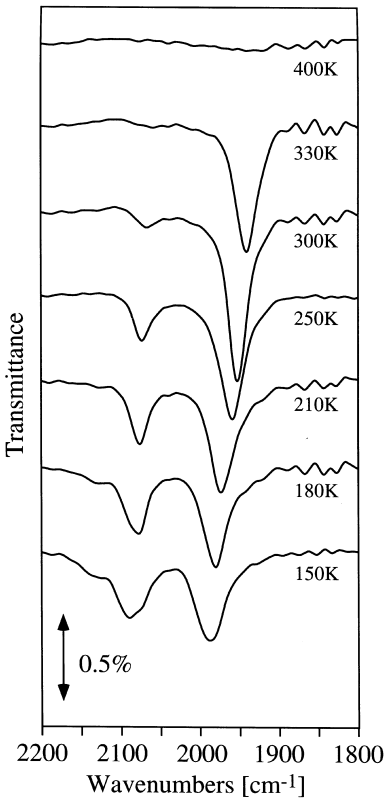

Fig. 8. The infrared spectra of CO adsorbed on palladium silicide grown at 400 K upon depositon of 2.4 ML Si and after annealing at the temperatures indicated.

uppermost spectrum in Fig. 7, indicating an analogous crystalline surface morphology to that upon Si deposition at 550 K. The following series shows spectra of the remaining CO at the indicated annealing temperatures. The CO molecules adsorbed on the unreacted Si are the first desorbing species. This is evident in the disappearing high-frequency shoulder at 2104 cm^{-1} at temperatures between 150 and 210 K (see also Fig. 1, topmost spectrum). Upon further annealing the intensities of the remaining two absorptions at 2074 and 2000 cm^{-1} decrease slowly. Complete desorption takes place above 300 K, a temperature which roughly coincides with the measured desorption of CO from the Pd(110) surface [25]. The binding of CO to the crystalline silicide is obviously much stronger compared to CO bound to a-Si, and resembles more the adsorption of CO on metallic surfaces.

As a structure model for crystalline palladium silicide, we propose the schematic model presented at the right-hand side of Fig. 9. The Pd substrate atoms are represented by grey spheres arranged in chains running along the $[\bar{1}10]$ direction of the substrate. The silicide unit cell is indicated by the straight lines. Only one single domain is presented. Its preferred growth direction is the $[\bar{1}1\bar{2}]$ direction. The incorporated Si atoms (black spheres) are located in the troughs between adjacent Pd chains occupying threefold adsorption sites. This arrangement is chosen in order to give the most uniform distribution of Si with an equal spacing between Si atoms. In addition, the structure satisfies the experimentally determined LEED pattern. The reason why we exclude a major rearrangement of Pd atoms to form the crystalline silicide is based on the following simple calculation: taking the relaxation in the z direction into account, the volume of the silicide unit cell becomes $V_{\text{silicide}} \approx 4 \times (2.75 \times 3.89 \times 1.29) \times 1.3\ \text{Å}^3 = 71.76\ \text{Å}^3$, which is approximately twice the volume of a Pd_2Si molecule ($V_{Pd_2Si} = 42\ \text{Å}^3$). Therefore, the most simple way to obtain two Pd_2Si molecules per silicide unit cell already containing four Pd atoms is simply to add two Si atoms.

The proposed structure is also consistent with the RAIRS results obtained for CO adsorbed on crystalline silicide. Several possible mechanisms are proposed to account for the frequency shift of the CO stretch vibration as a consequence of coadsorption [33,34]. The most popular models are an indirect surface-mediated interaction via a change in charge density or a direct interaction (overlap), often connected to a change of the adsorption geometry. Fig. 9 indicates the positions of CO on a pure Pd(110) surface (white spheres). Obviously, one quarter of the adsorbed molecules are directly affected by an overlap with the incorporated Si atoms, accounting for the second adsorption band at 2074 cm^{-1}. Its intensity will amount to about 25% of the whole spectrum, in good agreement with the experimental data. The most likely adsorption configurations into which the CO molecule may be forced due to the presence of Si in the surface layer are a threefold adsorption

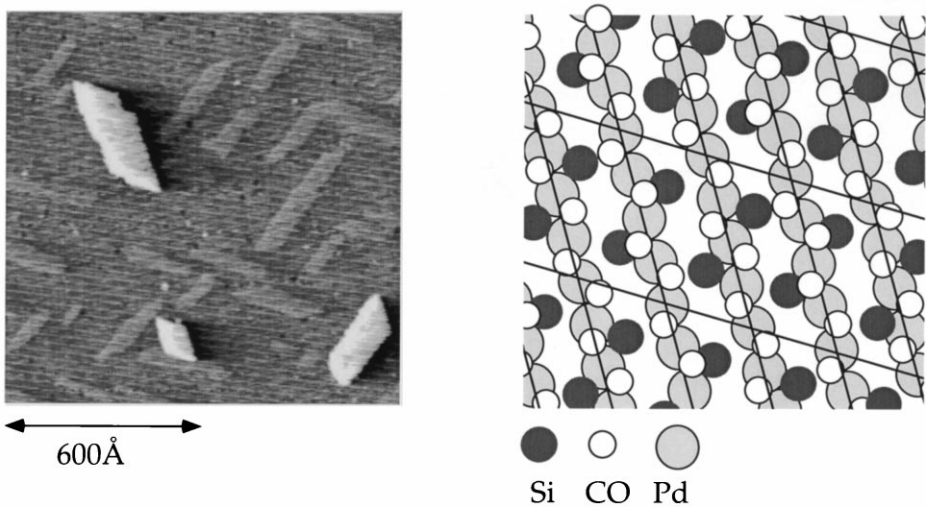

Fig. 9. Right: hard-sphere model of a monolayer of crystalline Pd_2Si grown on the Pd(110) surface. The grey spheres indicate Pd atoms forming chains running along the [$\bar{1}$10] direction of the substrate. The arrangement of dark spheres indicating Si atoms in the silicide layer corresponds to the experimentally obtained LEED pattern. The position of the CO molecules (white spheres) corresponds to the zig-zag chains observed on pure Pd(110). Left: STM images showing the surface morphology of crystalline palladium silicide after 0.4 ML Si deposition at 400 K.

site over two Pd atoms and one Si atom, a bridge-bound CO molecule above a mixed Si–Pd adsorption site or a CO molecule in an on-top position over a Pd atom in the silicide. All of these configurations are consistent with the appearance of a second absorption, and thus an unambiguous assignment of the 274 cm^{-1} mode of CO on palladium silicide is not possible.

3.3. *Metastability of the crystalline silicide*

The crystalline silicide formed on the Pd(110) surface is not stable at elevated temperatures. This is most evident by comparing the two STM images presented in Fig. 10, showing the surface morphology after 0.8 ML Si deposition at 550 K. The STM image in Fig. 10a was taken after quenching the sample to $T=400$ K immediately after Si deposition. Large embedded islands are clearly visible, and are typical of silicide formation at $T=550$ K. In contrast, the STM image on the right-hand side shows the corresponding surface morphology when keeping the sample at 550 K for about 30 min before imaging the zone. The surface is free of crystalline silicide islands: only the faceted form of the terrace step edges resembles the original silicide formation [29]. Obviously the silicide islands decompose on a minute timescale at 550 K. We also followed silicide decomposition in situ at 500 K, where it takes $\sim$2 h. With increasing time, the embedded silicide islands become smaller, and in addition the number of holes in the surface drastically increases. These holes are also visible at 550 K, and are stable during the STM measurements (see Fig. 10b). The large-scale image in Fig. 10b shows no hints of 3D clusters on the terraces or at step edges. We have scanned many different zones, and always observed simlar flat Pd terraces with small holes. Coarsening of the crystalline silicide into 3D clusters at the surface can thus be excluded.

The RAIR spectra of Fig. 11 give further evidence that the dissolution of the silicide is not a local effect associated with the limited image field of the STM. The bottom spectrum shows the absorption spectrum of CO adsorbed on Si/Pd(110) which was prepared at 550 K and held at this temperature for 1 h. It shows a single absorption band at 2000 cm^{-1}, indicating the exclusive adsorption of CO on Pd sites. In the spectral region between 2074 and 2104 cm^{-1} no absorption bands, due to crystalline silicide, amor-

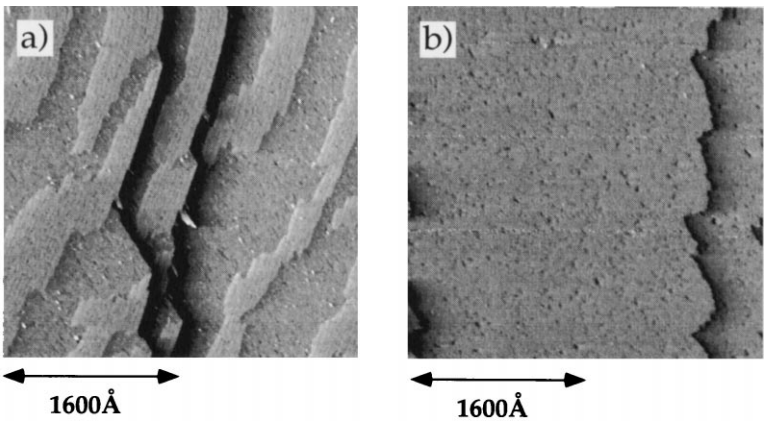

Fig. 10. The growth and dissolution of crystalline palladium silicide upon 0.8 ML Si deposition at 550 K. The STM image in (a) was taken immediately after deposition (the surface was quenched to 400 K), whereas the STM image in (b) was taken 60 min after deposition while keeping the temperature at 550 K.

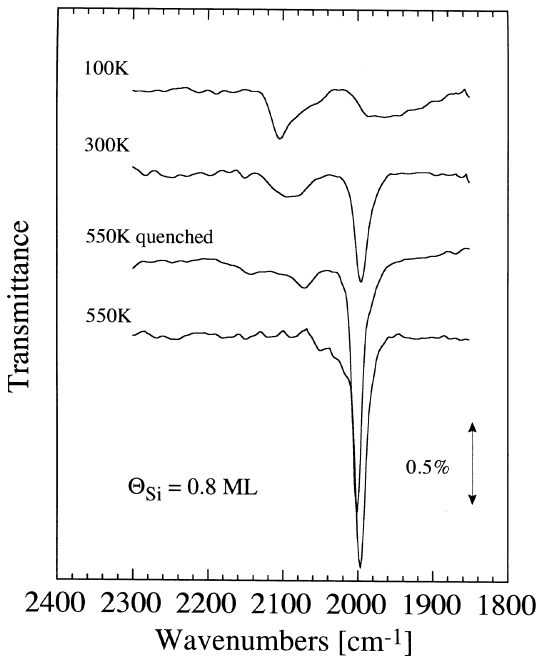

Fig. 11. Infrared absorption spectra of a monolayer of CO adsorbed on Si/Pd(110) after 0.8 ML Si deposition at 100, 300, 550 (the surface was quenched to 400 K after deposition) and 550 K (the surface was kept at 550 K for 60 min). 40 L CO was dosed on the surface at 100 K.

phous silicide or a-Si, are observed. Thus, the vibrational spectra demonstrate that the entire surface is completely Pd-terminated. We must conclude that the Si atoms which are released during silicide decomposition diffuse subsurface and are buried below the surface [29]. The randomly distributed holes in the topmost layer are the signature of this subsurface diffusion process.

Subsurface diffusion of Si on Pd(110) is already active even before silicide decomposition becomes significant. Fig. 12 shows the surface area covered

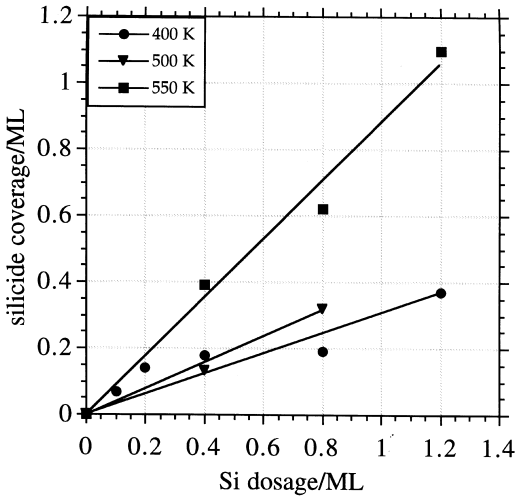

Fig. 12. The surface area covered with crystalline silicide as a function of Si dosage at the three different deposition temperatures: ● $T=400$ K, ▼ $T=500$ K, ■, $T=550$ K. Obviously, the formation of crystalline silicide at the surface is temperature-dependent, and is most pronounced at 550 K.

with crystalline silicide as a function of Si dosage for three different deposition temperatures. The Si/Pd(110) surfaces were quenched to 400 K directly after preparation and before taking the STM images. Obviously the amount of silicide which is formed at the surface is dependent on the temperature. In general, we observe a pronounced increase in silicide formation over subsurface diffusion with increasing temperature. The reaction scenario at the Si/Pd(110) interface can be described qualitatively by the reaction scheme

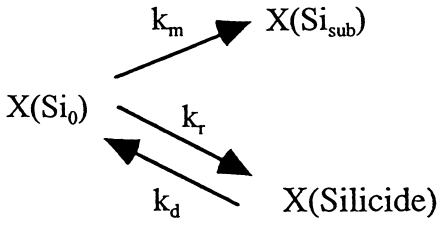

where $X(\mathrm{Si})$ denotes the concentration of Si on the surface ($X(\mathrm{Si_0})$), of Si in the Pd substrate ($X(\mathrm{Si_{sub}})$) and of the concentration of silicide at the surface ($X(\mathrm{Silicide})$). The temperature dependent miscibility of Si in the Pd substrate is treated as a second reaction channel in addition to the most obvious one, i.e. the surface silicide reaction. As all processes (chemical reaction, decomposition and subsurface diffusion) are thermally activated, the corresponding reaction rates (k_i) depend exponentially on their activation barriers. At very low temperatures, all reaction channels are frozen and unreacted Si nucleates at the surface. With increasing temperature, the reaction channel with the lowest energy barrier becomes populated first. After reaching a certain temperature, the higher energy barrier can also be overcome, and population into the second channel will be observed. Since the nucleation of embedded silicide islands is only possible by Si atoms being incorporated in the substrate, it is natural to assume that the barrier for interdiffusion is lower than the chemical activation energy for silicide formation. The pronounced formation of surface silicide at 550 K confirms this assumption (see Fig. 11). If we neglect silicide decomposition, the ratio between $X(\mathrm{Si_{sub}})$ and $X(\mathrm{Silicide})$ would be independent of time, and the experimental data of Fig. 11 would directly reveal a measure of the difference between the energy barriers of subsurface Si diffusion and silicide reaction. The crystalline silicide is unstable at elevated temperatures, indicating the thermal activation of silicide decomposition. After decomposition of the entire silicide islands, a flat Pd-terminated surface is left. Thus, the energetic ground state of the system is the mixing of Si in the selvedge of the Pd substrate.

The simple reaction model allows a rough estimate of the involved activation barriers for subsurface diffusion (E_m), for crystalline silicide reaction (E_r) and decomposition (E_d). Let us assume a rate constant k_i following Arrhenius behaviour, i.e. $k_i = f \sim \exp(E_i/kT)$. For simplicity, the frequency factor f is assumed to be equal for the different reaction channels i: $f = 1 \times 10^{13}\ \mathrm{s}^{-1}$. First, amorphous silicide is formed at the Pd(110) surface. The formation temperature of $T = 140$ K indicates a very low energy barrier E of $E \approx 0.35$ eV. The crystallisation temperature for silicide is ~ 320 K. Already at 320 K, small but well-shaped crystalline silicide islands are detected on the Pd(110) surface. Thus, the barrier for crystallisation is estimated to be $E_\mathrm{r} \approx 0.9$ eV. The barrier for subsurface diffusion is assumed to be smaller, i.e. $E_\mathrm{m} < E_\mathrm{r}$. The energy barrier for decomposition can be estimated considering the lifetime ($t_{1/2} = \ln 2/k_\mathrm{d}$) of the silicide islands as a function of temperature. Assuming lifetimes of $t_{1/2} = (550\ \mathrm{K}) \approx 600$ s and $t_{1/2}(500\ \mathrm{K}) \approx 8400$ s, an energy barrier for decomposition of $E_\mathrm{d} \approx 1.7$ eV is inferred. Although these estimates of the activation barriers are quite rough, they provide a valuable guide to understand the kinetics of silicide formation at the Pd(110) surface.

4. Conclusion

The nucleation and growth of silicide during the deposition of Si on Pd(110) has been studied. The experimental results reveal that silicide formation upon Si deposition on Pd(110) is similar to silicide formation upon Pd deposition on Si substrates. The growth scenario in both systems depends strongly on the deposition temperature. The Si–Pd interface is extremely reactive: silicide reaction

occurs at $T \leq 180$ K. With increasing temperature, initially amorphous silicon ($T < 140$ K) and then amorphous silicide ($T = 140$–320 K) grows at the metal surface. The CO stretch vibration has been shown to be very sensitive to the local bonding arrangement on the heterogeneous Si/Pd(110) surface. The infrared absorption of CO adsorbed at the three-dimensionally grown Si is centred at 2104 cm^{-1} and identical to CO adsorbed on thick amorphous Si films. Reactive Si deposition on the Pd(110) surface is accompanied by a considerable red-shift of the CO absorption band, indicating the formation of palladium silicide at the surface.

The main difference between the two systems (i.e. silicon on palladium and palladium on silicon) is the structure of the grown crystalline silicide and its crystallisation temperature. Whereas on Si substrates only amorphous Pd_2Si is observed upon Pd deposition below ~ 600 K, we have shown that at temperatures slightly above room temperature the Pd(110) substrate promotes the growth of a crystalline silicide phase.

The crytalline structure of the thermodynamically stable Pd_2Si is hexagonal, with a lattice constant of 6.5 Å in the basal plane and 3.4 Å in the z direction. In contrast to the Pd/Si(111) system, no epitaxial condition connects this unit cell with the rectangular surface unit cell of Pd(110). Consequently, the $\begin{pmatrix} 1 & 1 \\ 4 & 0 \end{pmatrix}$ LEED superstructure of epitaxially grown silicide on Pd(110) does not coincide with the geometry of the hexagonal unit cell of Pd_2Si. The silicide islands in the STM images of Figs. 4 and 9 nicely reflect the rhombic structure of the unit cell. Both domains are clearly visible. The silicide islands represent a metastable crystalline phase of palladium silicide grown epitaxially on the Pd(110) surface. This finding is not surprising, since palladium silicide is known to be a very transformable alloy. In bulk–bulk reaction studies, up to seven different metastable crystalline palladium silicide phases, enumerated from MSA to MSG, have already been observed [35,36]. Other silicide systems also demonstrate metastable phases. The closely related iron silicide exhibits the most well studied metastable $FeSi_{1+x}$ phases crystallising on the Si(111) surface [37]. In heterogeneous metal-on-metal epitaxial systems, it is known that strain due to a significant lattice mismatch might work as driving force for the formation of metastable crystalline structures [38–40].

The crystalline palladium silicide formed on Pd(110) is unstable at elevated temperatures. After decomposition of the entire silicide islands, a flat Pd-terminated surface is left. A temperature-dependent miscibility of Si in the selvedge of the Pd substrate is proposed to account for this finding.

Although there are subtle differences in the behaviour of the Pd–Si and the Si–Pd(110) systems, as discussed above, both interfaces spontaneously produce Pd_2Si at temperatures above 150 K, suggesting a relatively small chemical reaction barrier. The chemical compound formed is rather insensitive to the nature of the substrate. Obviously, the interpenetration of atoms at both interfaces is sufficient to ensure complete mixing in the initial phase of interface formation. For the Si–Pd system this is somewhat surprising, as Si penetration in the metal has not been considered until recently. It is the delicate competition between Si subsurface diffusion and silicide formation which is at the origin of the rich temperature-dependent growth scenario. The structures of the crystalline silicides, on the other hand, reflect much more the microscopic environment of the different interfaces. While the Si(111) surface can accommodate a stable Pd_2Si phase, the substantial strain at the Pd(110) interface renders the silicide unstable.

References

[1] V.B. Lifshits, A.A. Saranin, A.V. Zotov, Surface Phases on Silicon: Preparation, Structures and Properties, Wiley, New York, 1994.
[2] J.M. Poate, K.N. Tu, J.W. Mayer, Thin Films – Interdiffusion and Reactions, New York, 1978.
[3] A. Franciosi, D.W. Niles, G. Margaritondo, C. Quaresima, M. Capozzi, P. Perfetti, Phys. Rev. B 32 (1985) 6917.
[4] K. Nishimori, H. Tokutaka, H. Sumi, N. Ishihara, J. Vac. Soc. Jpn. 34 (1991) 134.
[5] M.A. Chester, A.B. Horn, J. Phys. Condens. Matter 3 (1991) 251.
[6] M.C. Munoz, F. Soria, J.L. Sacedon, Surf. Sci. 189/190 (1987) 204.

[7] R. Dudde, H. Bernhoff, B. Reihl, Phys. Rev. B 41 (1990) 12029.
[8] J.A. Martin-Gago, R. Fasel, J. Hayoz, R.G. Agostino, D. Naumovic, P. Aebi, L. Schlapbach, Phys. Rev. B 55 (1997) 12896.
[9] M.W. Ruckman, J.J. Joyce, F. Boscherini, J.H. Weaver, Phys. Rev. B 34 (1986) 5118.
[10] S. Okada, K. Oura, T. Hanawa, K. Satoh, Surf. Sci. 97 (1980) 88.
[11] G. Majani, F. Nava, G. Ottaviani, E. Donna, G. Leggieri, A. Luches, G. Celotti, J. Appl. Phys. 52 (1981) 4055.
[12] L. Casais, C. Casati, R. Rosei, M. Kiskinova, Surf. Sci. 331–333 (1995) 381.
[13] A.A. Kuznetsov, S.Y. Abramova, T.E. Potapova, O.D. Protopopov, J. Electron Spectrosc. Relat. Phenom. 68 (1994) 407.
[14] C.M. Comrie, J.M. Egan, J. Appl. Phys. 64 (1988) 1173.
[15] N.W. Cheung, M.-A. Nicolet, M. Wittmer, C.A. Evans, T.T. Sheng, Thin Solid Films 79 (1981) 53.
[16] G.E. White, H. Chen, J. Appl. Phys. 68 (1990) 3317.
[17] M. Wittmer, K.N. Tu, Phys. Rev. 27 (1983) 1173.
[18] U.K. Köhler, J.E. Demuth, R.J. Hamers, Phys. Rev. Lett. 60 (1988) 2499.
[19] S. Kawamoto, K. Saitoh, M. Hirai, M. Kusaka, M. Iwami, Surf. Sci. 287/288 (1993) 151.
[20] G.W. Rubloff, P.S. Ho, J.F. Freeouf, J.E. Lewis, Phys. Rev. B 23 (1981) 4183.
[21] R.M. Tromp, E.J. von Loene, M. Iwami, R.G. Smeenk, F.W. Saris, F. Nava, G. Ottaviani, Surf. Sci. 124 (1983) 1.
[22] H. Roux, N. Boutaoui, M. Tholomier, Surf. Sci. 260 (1992) 1123.
[23] E. Hahn, A. Fricke, H. Röder, K. Kern, Surf. Sci. 297 (1993) 19.
[24] M.A. Chester, G.S. MacDougall, M.E. Pemble, N. Sheppard, Surf. Sci. 164 (1985) 425.
[25] E. Hahn, E. Kampshoff, K. Kern, Chem. Phys. Lett. 223 (1994) 347.
[26] A. Locatelli, B. Brena, S. Lizzit, G. Comelli, G. Cautero, G. Paolucci, R. Rosei, Phys. Rev. Lett. 73 (1994) 90.
[27] R. Raval, M.A. Harrison, D.A. King, Surf. Sci. 211/212 (1989) 61.
[28] Y. Bu, M.C. Llin, Surf. Sci. 298 (1993) 94.
[29] E. Kampshoff, N. Wälchli, K. Kern, Surf. Sci. 382 (1997) L705.
[30] A.K. Schmid, J.C. Hamilton, N.C. Bartelt, R.Q. Hwang, Phys. Rev. Lett. 77 (1996) 2977.
[31] P.S. Ho, G.W. Rubloff, J.E. Lewis, V.L. Moruzzi, A.R. Williams, Phys. Rev. B 22 (1980) 4784.
[32] G. Blyholder, J. Phys. Chem. 68 (1964) 2772.
[33] G. Pacchioni, P.S. Bagus, Chem. Phys. 177 (1996) 373.
[34] H. Yu, D.Q. Hu, K.T. Leung, Surf. Sci. 355 (1996) L335.
[35] L. Zongquan, H. Yizhen, Phys. Status Solidi (a) 98 (1986) 91.
[36] W. Xuehua, W. Zigin, Z. Shuyuan, Thin Solid Films 229 (1993) 33.
[37] H. von Känel, K.A. Mäder, E. Müller, N. Onda, H. Sirringhaus, Phys. Rev. B 45 (1992) 13807.
[38] Z.G. Wang, S.H. Lu, Y.S. Li, F. Jona, P.M. Marcus, Phys. Rev. B 35 (1987) 9322.
[39] H. Li, D. Tian, J. Quinn, Y.S. Li, F. Jona, P.M. Marcus, Phys. Rev. B 43 (1991) 6342.
[40] E. Hahn, E. Kampshoff, N. Wälchli, K. Kern, Phys. Rev. Lett. 74 (1995) 1803.